Nuclear Physics Applications in Astronaut Radiation Protection

Francis A. Cucinotta
University of Nevada, Las Vegas NV, USA

Presented at the
2018 European Nuclear Physics Conference
Bologna, Italy
September 5, 2018

UNLV School of ALLIED HEALTH SCIENCES
UNIVERSITY OF NEVADA, LAS VEGAS

Introduction

- New stochastic approaches to risk assessment are of interest to improve predictions of cancer and non-cancer risks, such as cognitive detriments, in galactic cosmic ray (GCR) risk assessments.
- To support new models for GCR risk assessment, stochastic radiation transport codes are needed, however long CPU times are a bottle-neck for space radiation applications:
  - Several weeks to transport all GCR primary and secondaries through spacecraft, Mars atmosphere, and tissue shielding.
  - Nuclear event generator a main cause of bottle-neck.
- We consider accuracy of nuclear models, including new data as published.
- To support new models for GCR risk assessment, “fast” accurate, stochastic radiation transport codes are needed.

GCR Energy Spectra

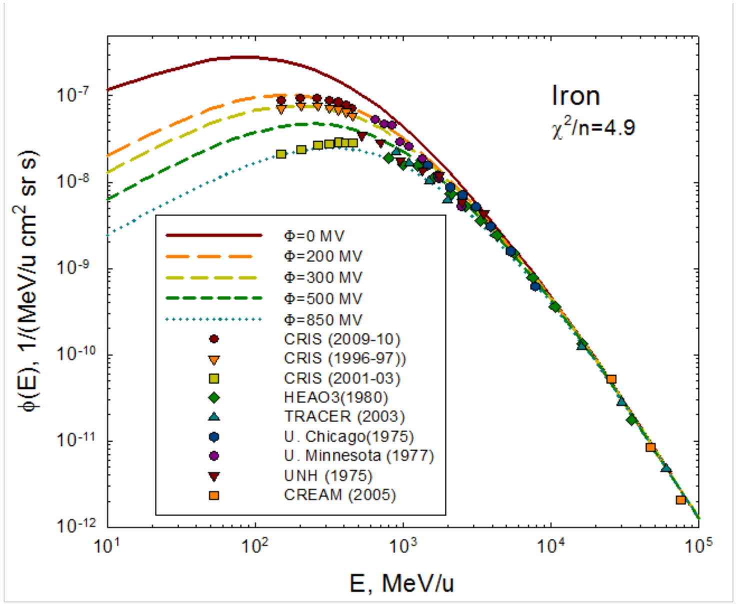

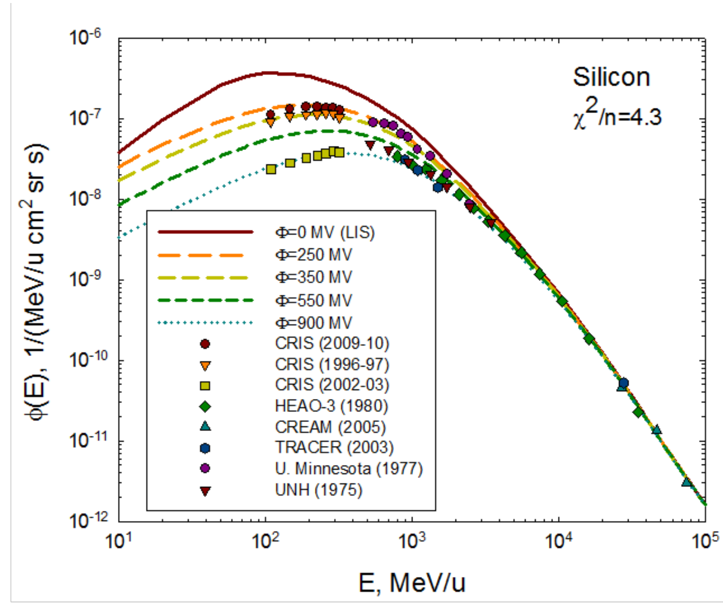

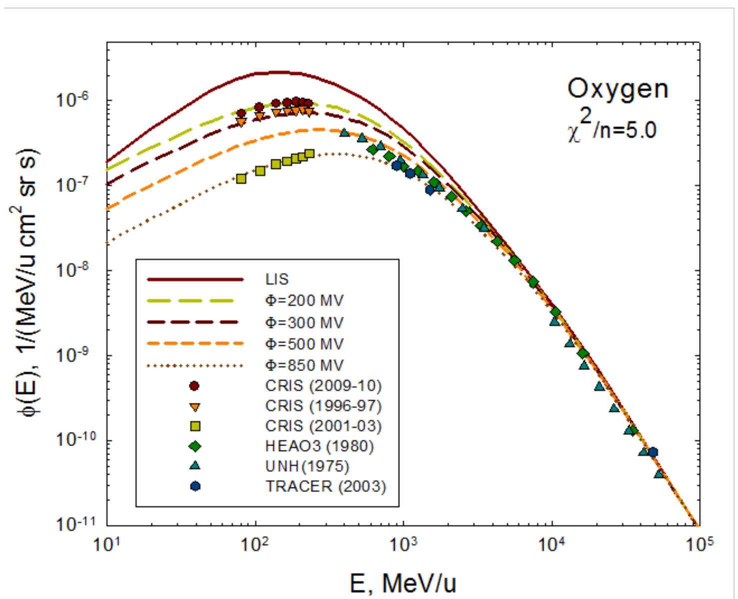

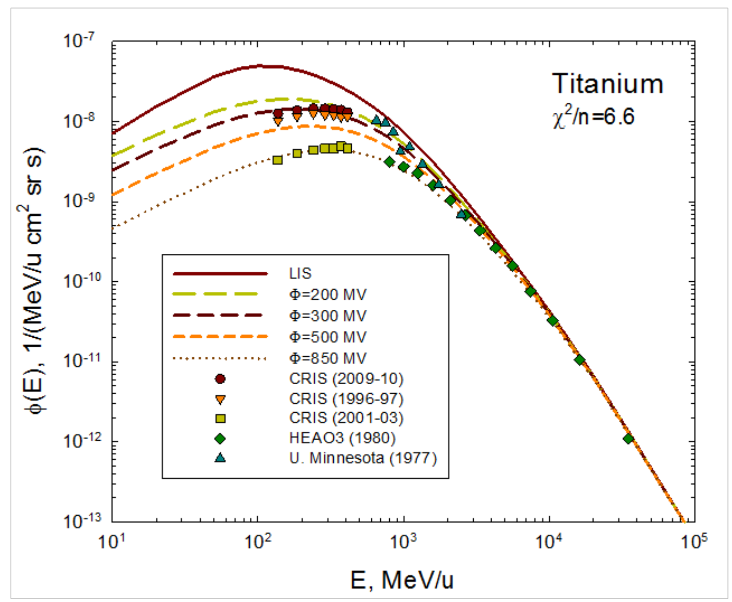

Comparisons of GERMcode to NRSL Data

^{28}Si (0.403 GeV/u) Bragg Curve and GERM Code

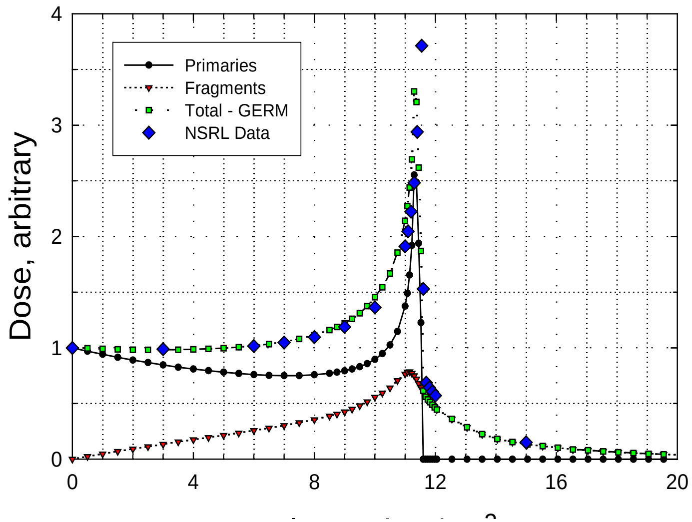

^{48}Ti (0.98 GeV/u) NSRL Bragg Curve vs GERM Code

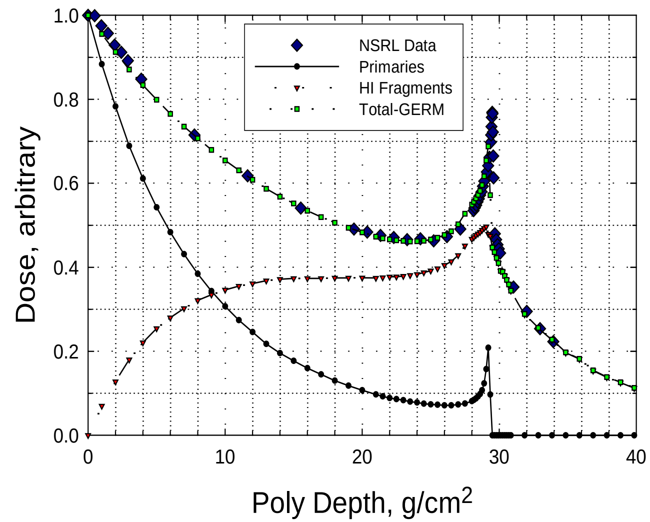

^{56}Fe(0.59 GeV/u) Bragg Curve and GERM Code

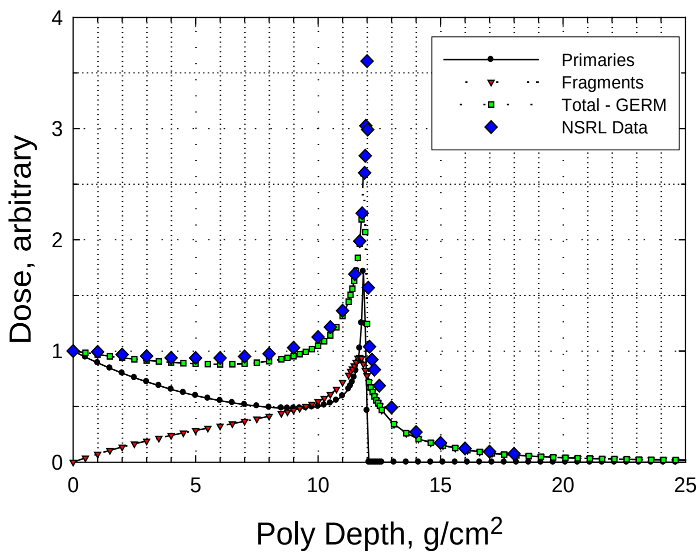

^{56}Fe(0.967 GeV/u) Bragg Curve and GERM Code

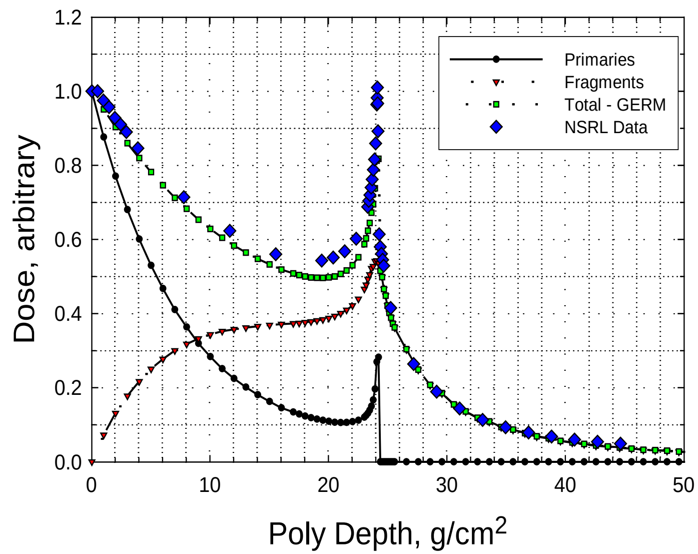

GERM Stochastic Event in Tissue: ^{56}Fe Beam

Stochastic events have important role in Energy deposition in tissue structures.

Iron (980 MeV/u) at Sample Depth (Flask)

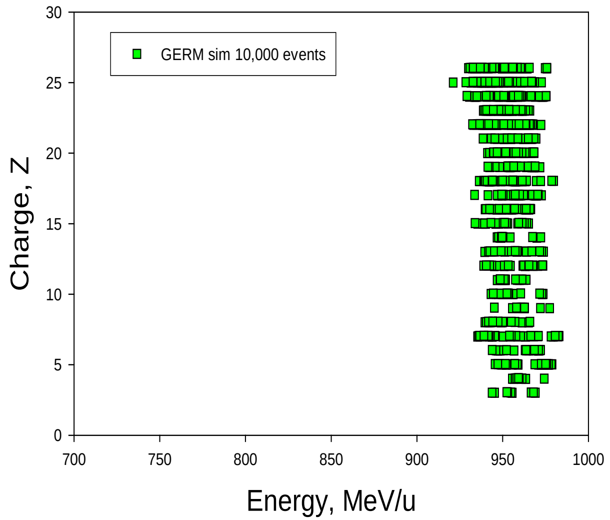

Iron (980 MeV/u) at 10 cm in Water Column

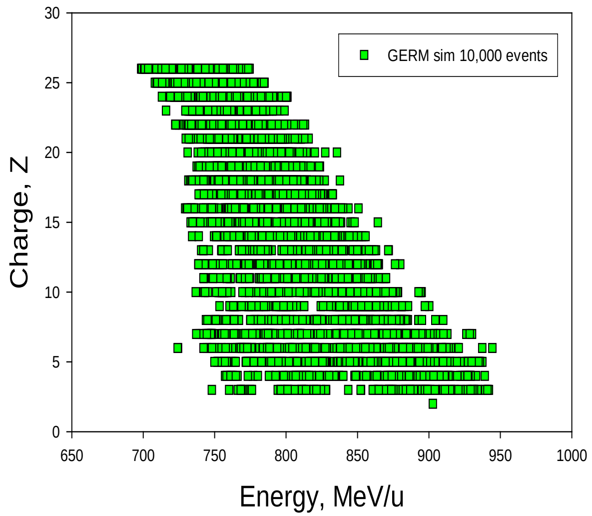

Iron (980 MeV/u) at 10 cm in Water Column

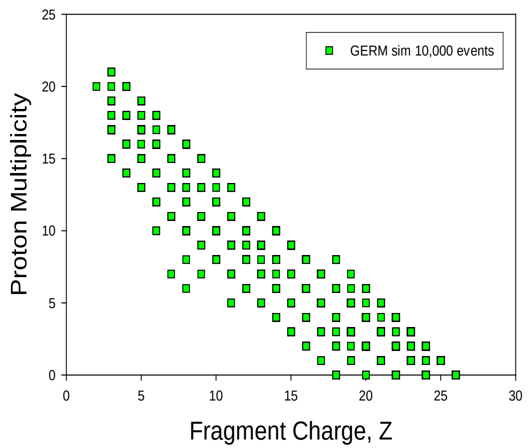

Iron (980 MeV/u) at 10 cm in Water Column

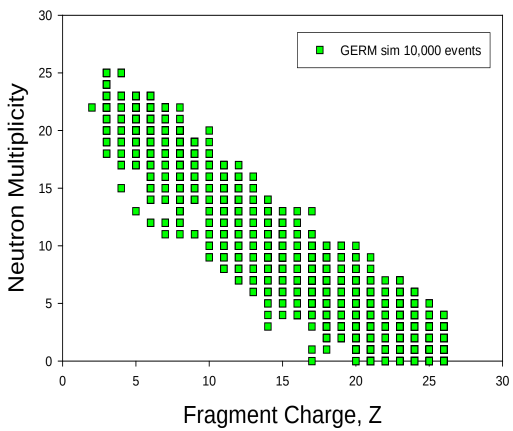

GCR effects on Cognition

Mouse hippocampus- neuron connectivity

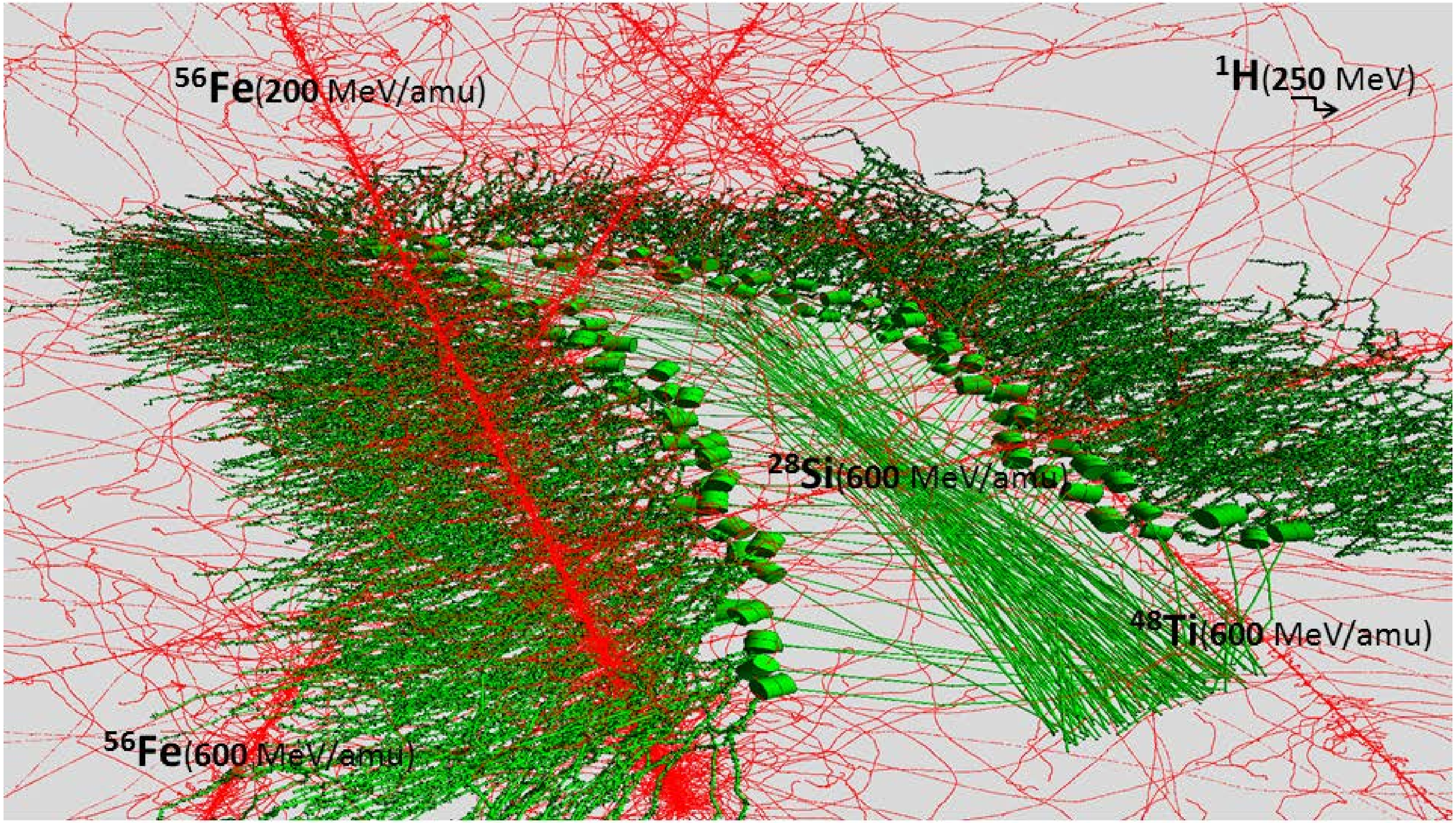

NASA Space Cancer Risk (NSCR) Model

- Reviewed by U.S. National Academy of Sciences (NAS) and NCRP:
  - 95% Confidence level for Limit of 3% Radiation Exposure Induced Death (REID).
    - Not conservative due to non-cancer risks yet to be evaluated
  - Radiation quality described using track structure theory.
    - PDF's for uncertainty evaluation
    - Leukemia lower Q than Solid cancer
  - Redefined age dependence of risk using BEIR VII approach.
    - UNSCEAR Low LET Risk coefficients
  - Risks for Never-Smokers to represent healthy workers.

GCR dominate ISS organ risk

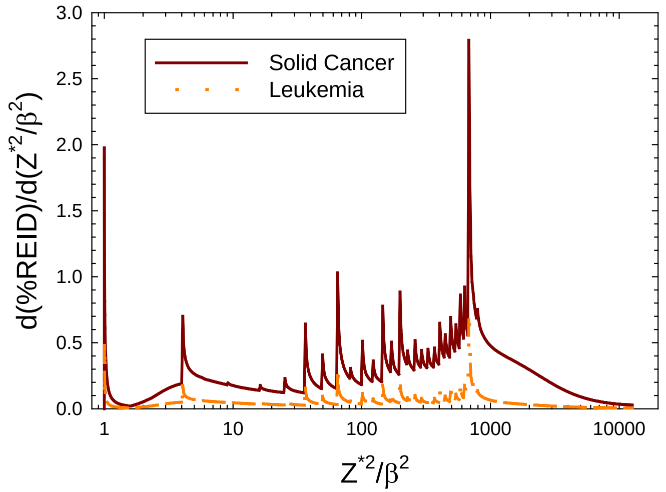

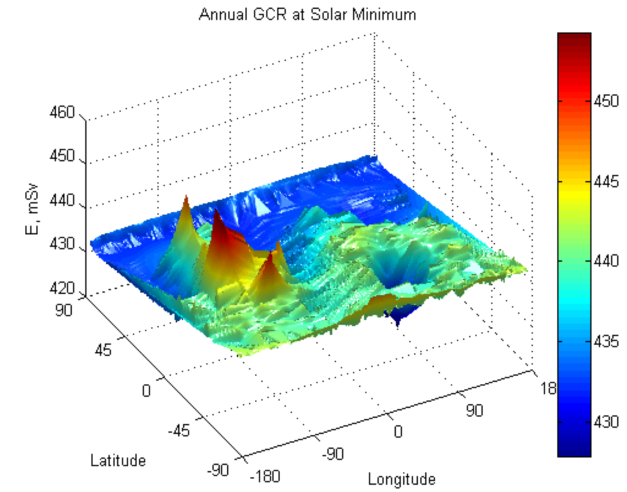

GCR doses on Mars

UNLV
UNIVERSITY OF NEVADA LAS VEGAS

Track Structure Approach of Radiation Quality Description: “core” and “penumbra” in Biological Effects

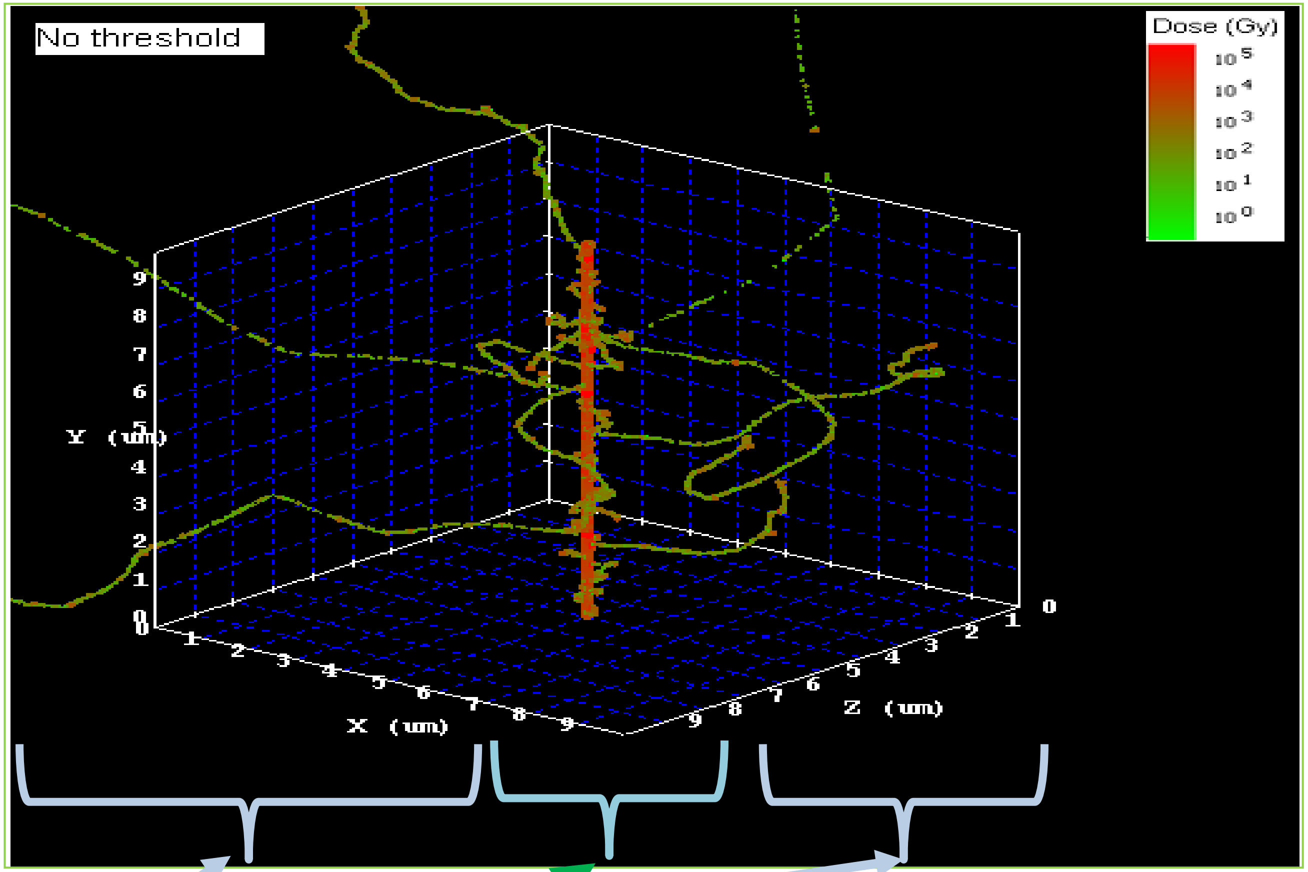

$$Q_{NASA} = (1 - P(Z,E)) + \frac{6.24(\Sigma_0 / \alpha_\gamma)}{LET} P(Z,E)$$

$$\frac{QF_{\gamma Acute}(Z,E)}{DDREF} = \frac{Q_{low}(Z,E)}{DDREF} + \overline{Q}_{high}(Z,E)$$

Improving NASA Quality Factor

based on mouse solid tumor RBE data for neutrons and HZE particles against Acute gamma-rays (lowers uncertainty)

RBE or QF for Fission neutrons are averaged over low energy proton, HI recoils etc. spectra.

Results suggest Fission neutrons and HZE Iron have similar RBEs and not max effective radiation.

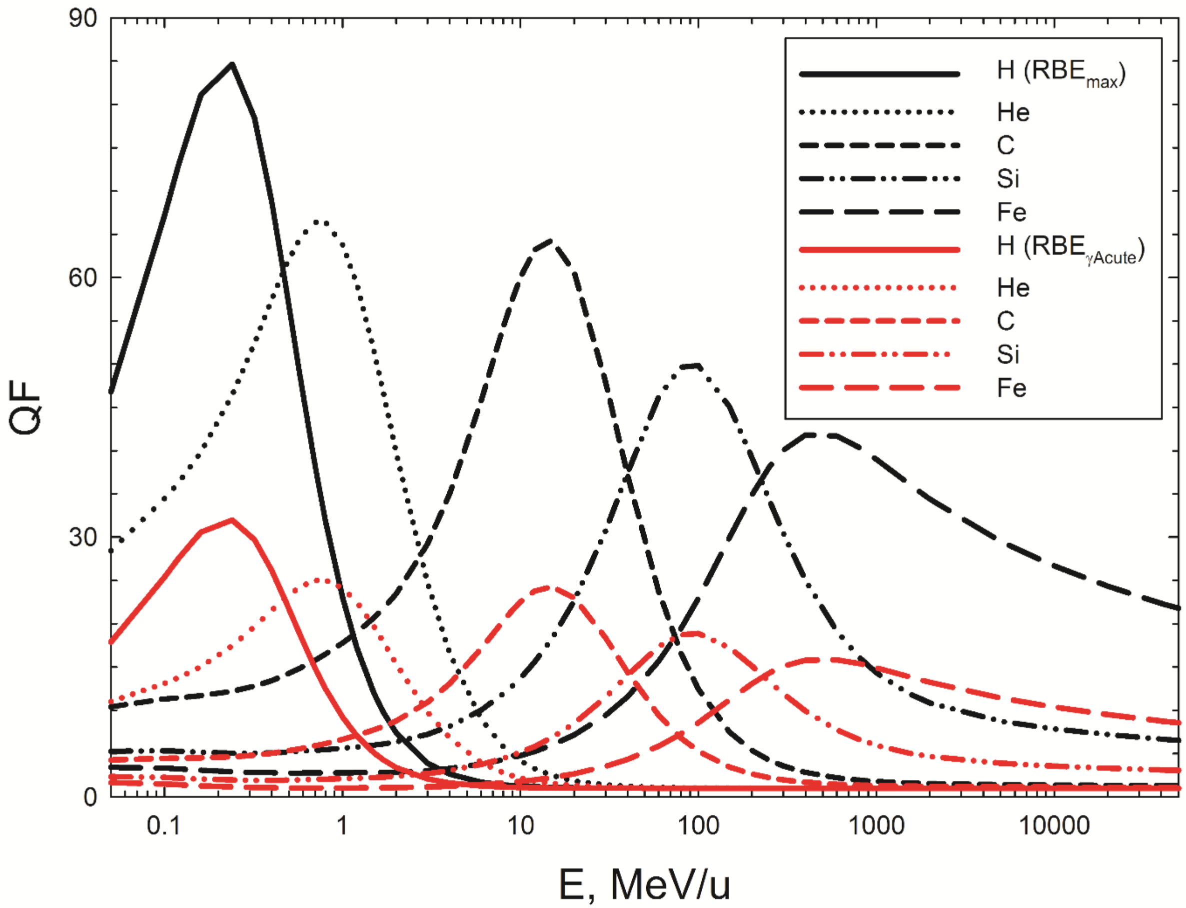

Cucinotta PloS One (2015)

QF of Z=1 is large in last cell layer:

Low E-protons produced in slowing down and from neutron elastic scattering.

Low E- pions produced predominantly in slowing down.

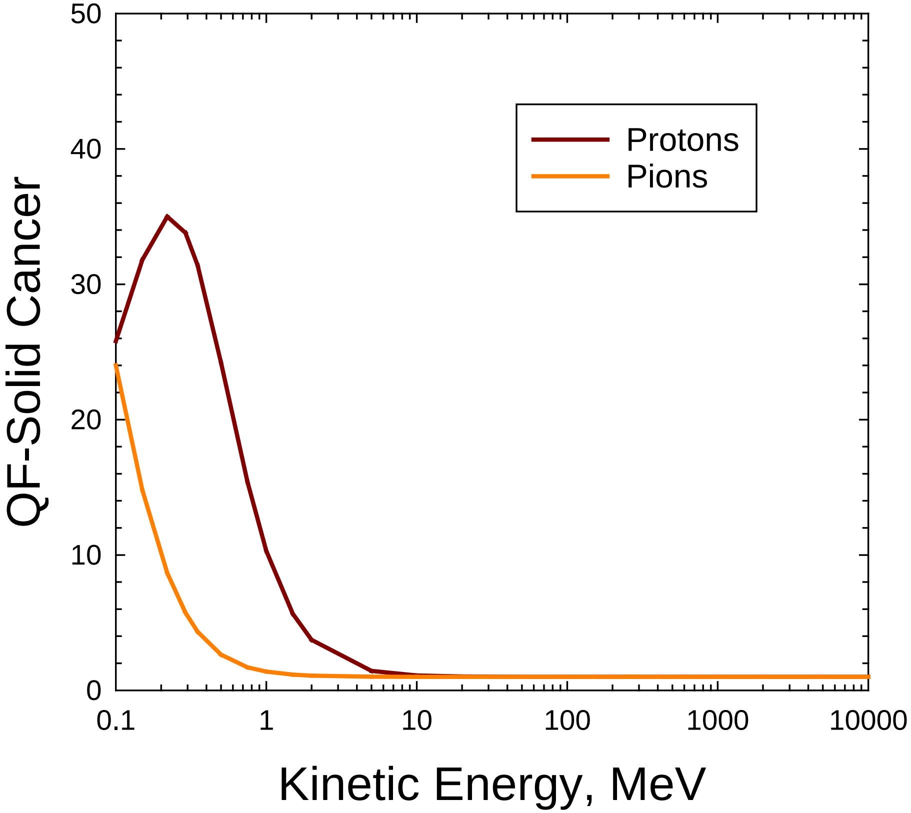

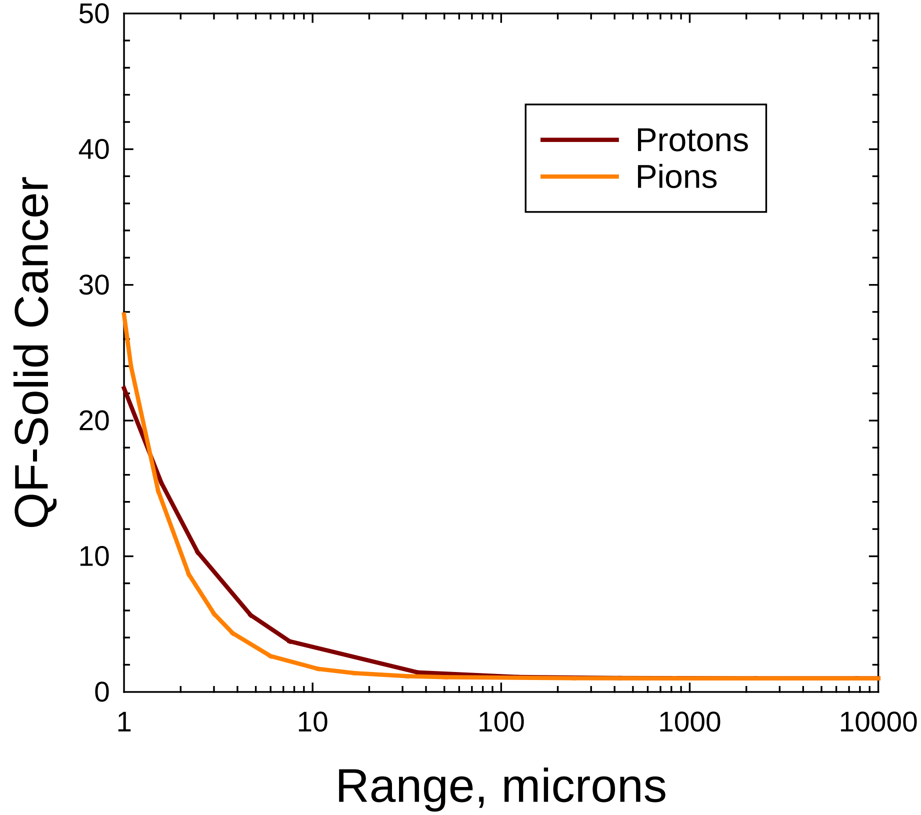

Integral Uncertainty Analysis

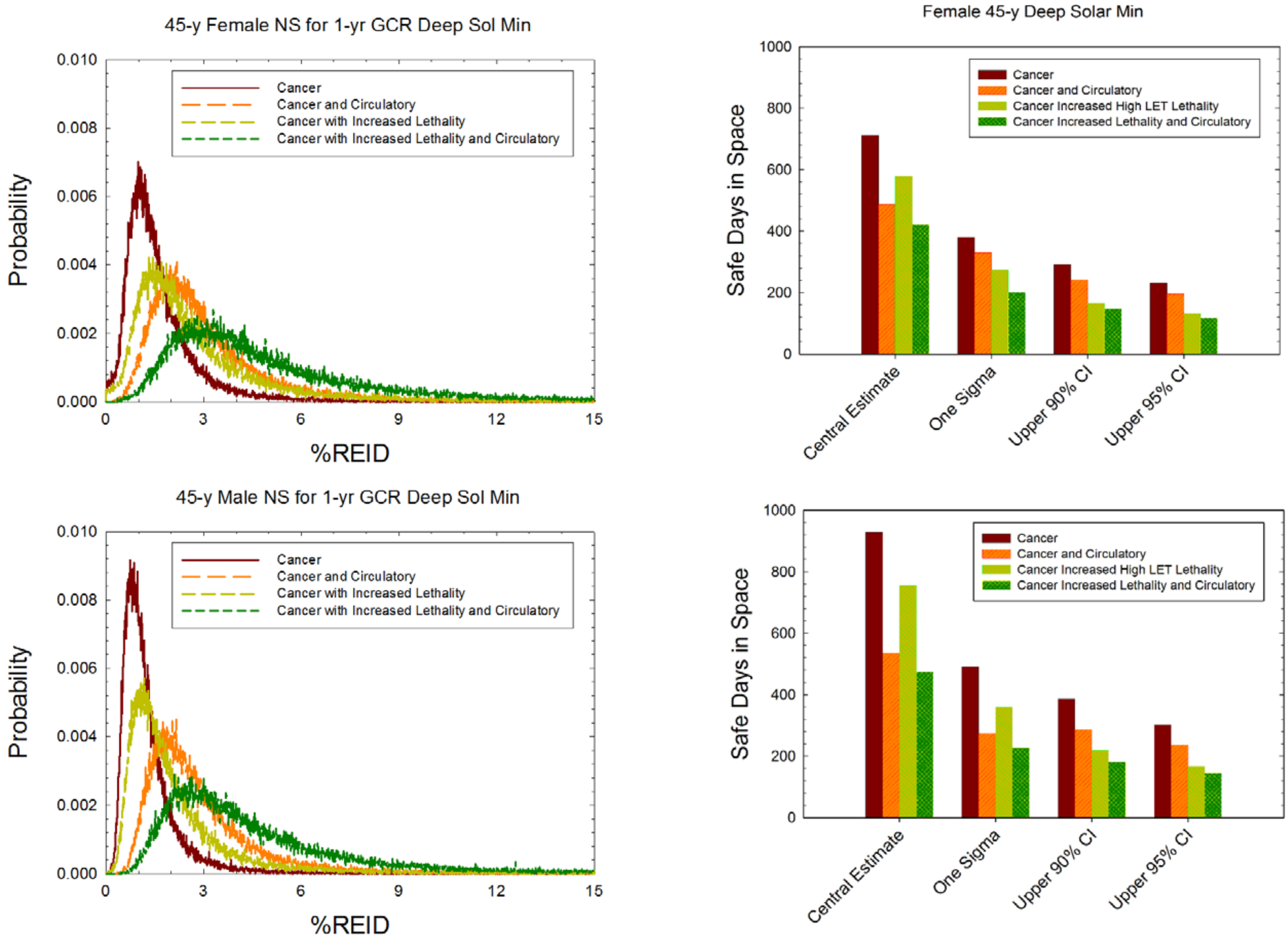

Cucinotta et al., Life Sci Space Res (2015)

Constraints on Nuclear Event-Generators

- Total Inelastic Cross Section.
- Heavy ion fragmentation cross sections.
- Distributions for light particle multiplicities ($n, p, {}^2H, {}^3H, {}^3He, {}^4He, \pi^{+/-}, \gamma, e^{+/-}, \mu^{+/-}$).
- Inclusive particle momentum distribution.
- Neutron elastic scattering.
- EM scattering cross sections.

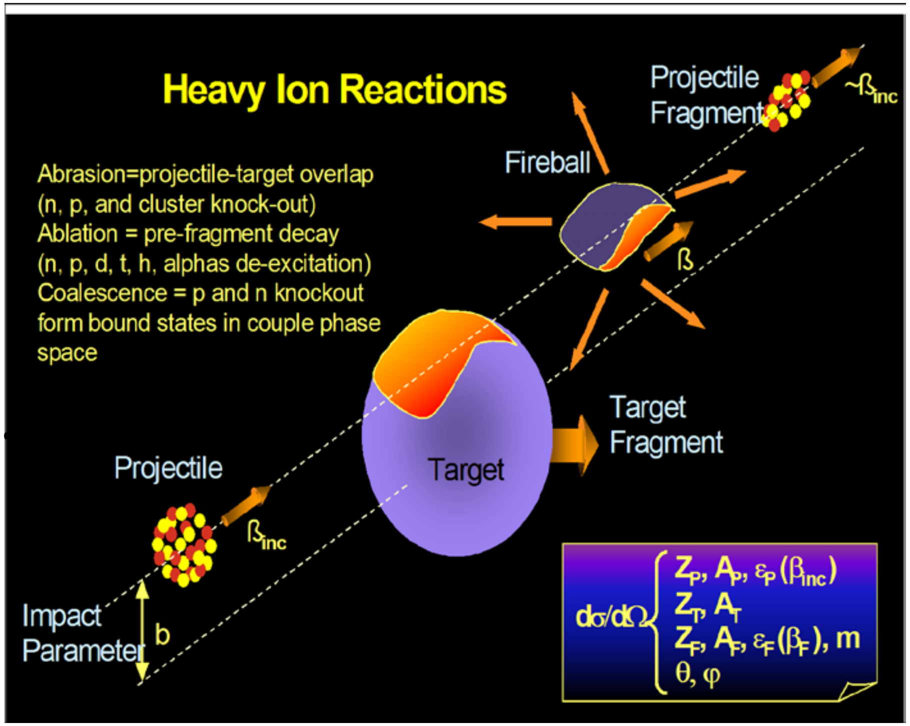

- Less well studied are 2-particle, 3-particle, … N-particle correlation functions from summing events.
- For heavy ions can be 5 contributions to an event (Projectile fragment, Target Fragments, Projectile like light particles, Target like light particles, and fireball contribution)

Systematic Approximations to HI Multiple Scattering Solutions

- Eikonal or Glauber Approximation.
- Coherent Approximation.
  - Intermediate state scattering stays in ground state (or single excited state) in forming final elastic (excited state)
- Optical Model Potential.
  - Formulate equivalent one-body equation
  - First-order Optical model assumes Coherent approximation
  - Second order optical model considers P and T two-body correlation function in first correction to coherent scattering, etc.
- Large mass limit.
- Pseudo-impulse approximation.
  - Use phenomenological medium modified two-body amplitudes
- Factorization Approximation for fragmentation.
  - Ignores some correlations
- Closure approximation (sum over all states of the unobserved piece (T, R, etc.)).

Absorption and Elastic Scattering

- Optical theorem $\sigma_{Total} = 4\,\pi/k\ \mathrm{Im}\,(f_{elastic}(q=0))$ (f like T)
- $\sigma_{Total} = \sigma_{Absorption} + \sigma_{Elastic}$
- Eikonal (Glauber) Approximation = forward angle approximation for total momentum transfer
  - Reduces Integral equations to Integrals (many particle)

$$g_{eik} = \left(\frac{\mathbf{k}\cdot(\mathbf{k}-\mathbf{k}')}{p_\alpha}\right)\delta\,(\mathbf{k}-\mathbf{k}')$$

$$\bar{f}(\mathbf{q}) = \frac{ik}{2\pi}\hat{Z}\int d^2b\, e^{i\mathbf{q}\cdot\mathbf{b}}\left\{e^{i\bar{X}(\mathbf{b})} - \bar{1}\right\}$$

$$\bar{X}(\mathbf{b}) = \sum_{\alpha,j}\frac{-\mu}{2k}\int_{-\infty}^{\infty} dz\, t_{\alpha j}\left(\mathbf{r}_\alpha - \mathbf{r}_j + \mathbf{x}\right)$$

$$X_{n\nu,n'\nu'}(\mathbf{b}) = \frac{-\mu}{2k(2\pi)^3}\sum_{\alpha,j}\int_{-\infty}^{\infty} dz\int d\mathbf{q}\ e^{i\mathbf{q}\cdot\mathbf{x}}\, F_{nn'}(-\mathbf{q})\, G_{\nu\nu'}(\mathbf{q})\, t_{\alpha j}(\mathbf{q})$$

2nd order elastic amplitude

$$f_{CC}^2(\mathbf{q}) \approx \frac{-ik}{2\pi}\int \exp(-i\mathbf{q}\cdot\mathbf{b})\left[\exp(iX_{EL})\cos\Upsilon - 1\right]d^2b$$

$$(6)\quad \Upsilon^2(\vec{b}) = \frac{A_P A_T}{(2\pi k_{NN})^2}\int d\vec{q}\,d\vec{q}'\,e^{i(\vec{q}+\vec{q}')\cdot\vec{b}}\cdot f_{NN}(-\vec{q}')\, f_{NN}(\vec{q})\sum_{n=1}^{5} y_n(\vec{q},\vec{q}')$$

$$\sigma_{ABS} = 2\pi\int_0^\infty b\,db\left\{1 - \frac{1}{2}\exp\left(-2\ \mathrm{Im}\ X_{EL}\right)\left[\cosh\left(2\ \mathrm{Im}\ \Upsilon\right) + \cos\left(2\ \mathrm{Re}\ \Upsilon\right)\right]\right\}$$

>Two-body Form Factors

Energy Dependence of Absorption:

Follows NN energy dependence, with nuclear medium and Coulomb corrections.

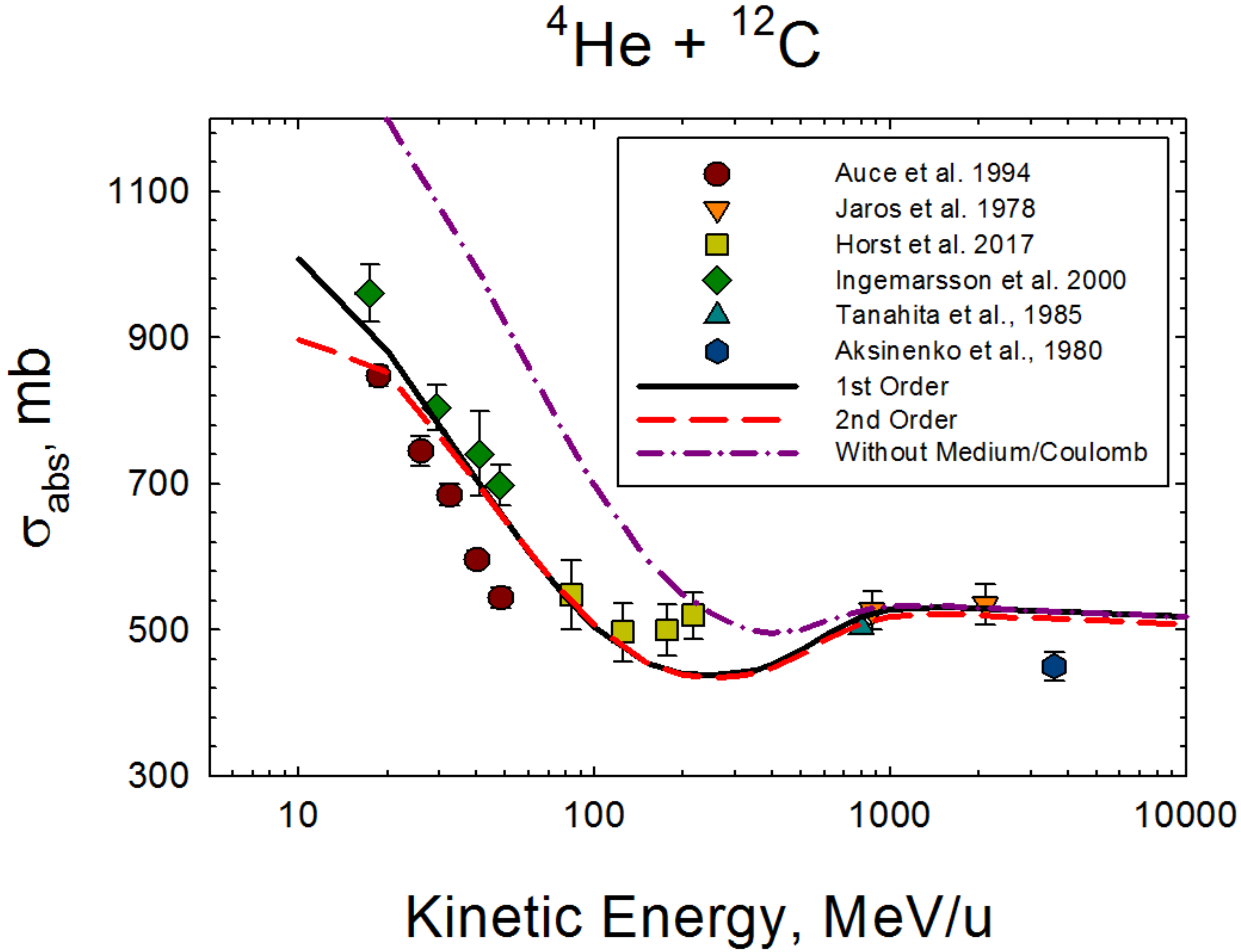

Pion Total Inelastic Cross Section

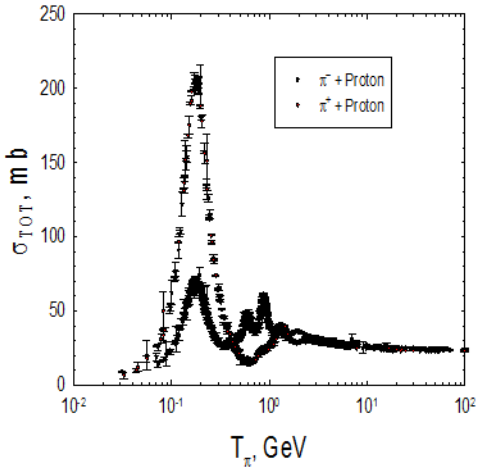

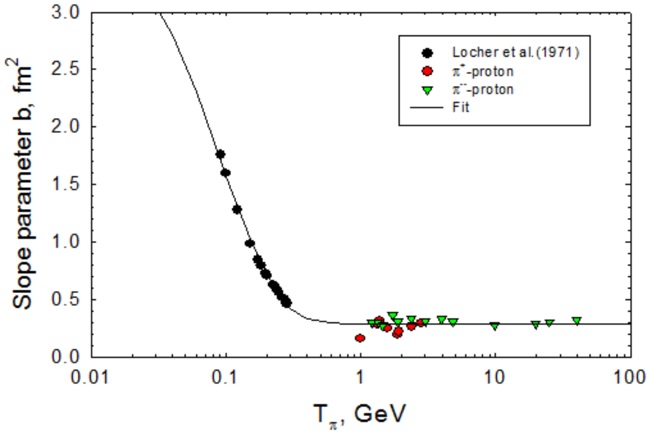

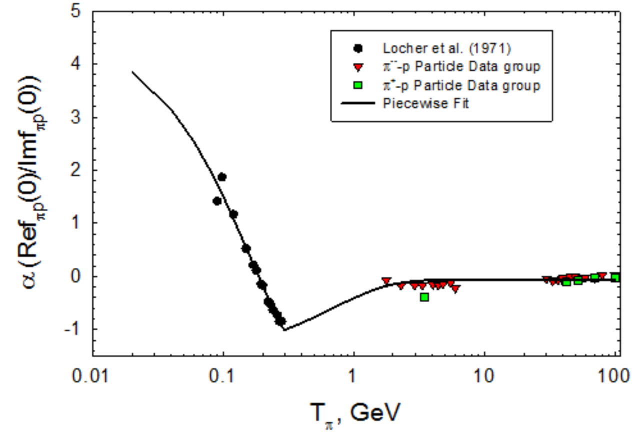

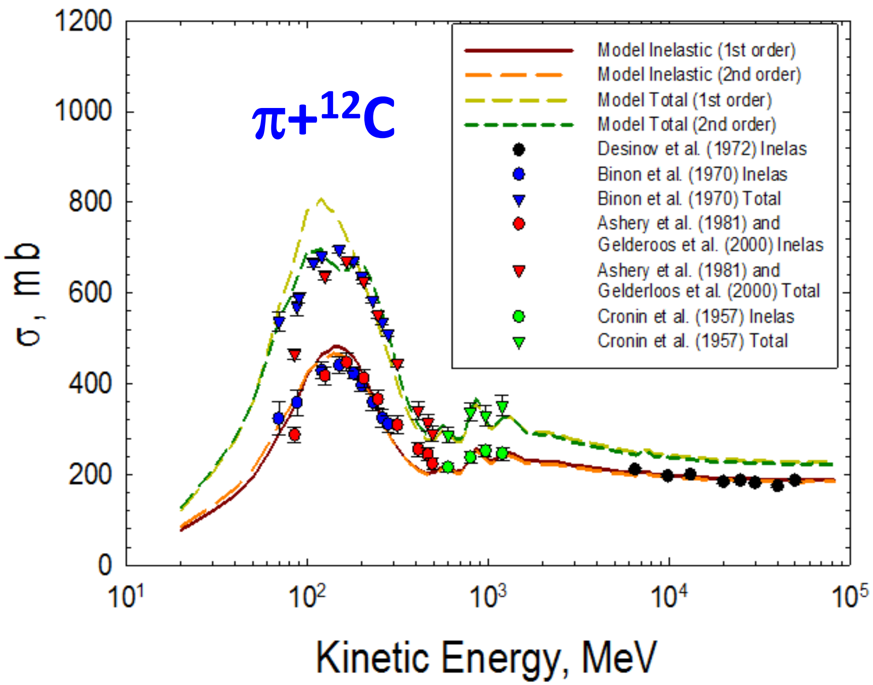

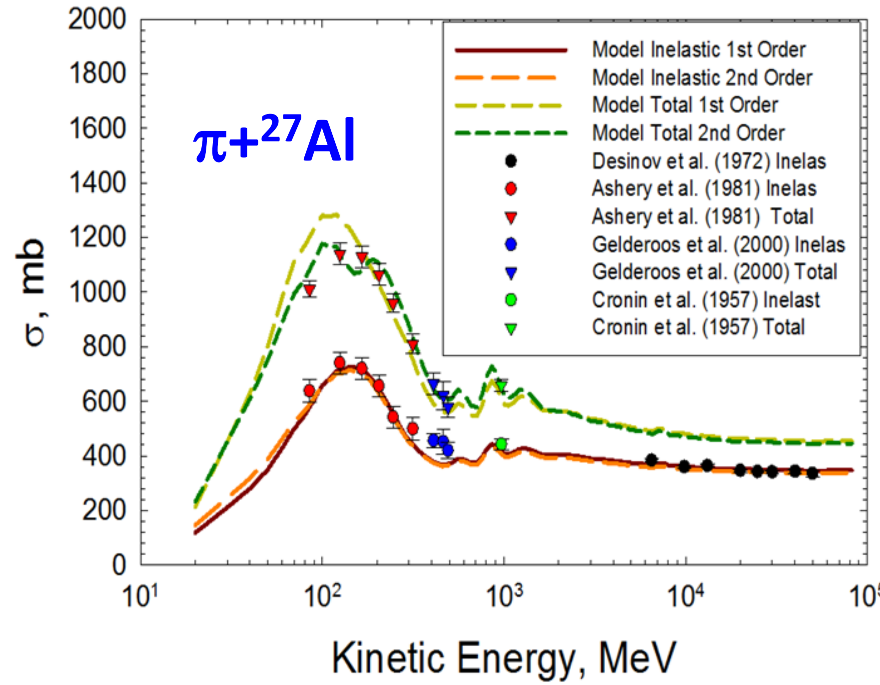

Predictions of absorption cross sections for projectiles on ^{12}C targets. Experimental errors are shown as the standard deviation (SD). %-differences between 1st-order and 2nd-order optical models with experiments are shown.

3a). Magnesium isotopes (Beam energy is 950 MeV/n).

A	Expt.	SD	Opt1	%Diff.	Opt2	%Diff.
20	1150	16	1191.4	-3.6	1150.4	-0.03
22	1170	33	1212.7	-3.7	1165.5	0.4
23	1208	68	1227.4	-1.6	1176.8	2.6
24	1136	72	1243.8	-9.5	1189.8	-4.7
25	1172	113	1263.7	-7.8	1206.0	-2.9
27	1203	16	1305.7	-8.5	1240.9	-3.2
29	1264	16	1352	-7.0	1278.8	-1.2
30	1301	8	1375.5	-5.7	1298.2	0.2
31	1335	35	1399.4	-4.8	1318.0	1.3
32	1340	24	1423.6	-6.2	1337.9	0.2
33	1393	254	1448	-4.0	1358.1	2.5

3b). Aluminum isotopes (Beam energy is 950 MeV/n).

A	Expt.	SD	Opt1	%Diff.	Opt2	%Diff.
23	1208	68	1221.2	-1.1	1172.1	3.0
24	1136	72	1232.9	-8.5	1180.4	-3.9
25	1158	74	1246.4	-7.6	1190.5	-2.9
26	1179	76	1261.1	-7.0	1201.5	-1.9
27	1200	78	1277	-6.4	1214.1	-1.2
28	1221	80	1316.8	-7.9	1229.8	-0.7

Cucinotta, Yan, Saganti Nucl Instrum Meth (2018)

Abrasion-Ablation Fragmentation Model

- P + T → F*+R+X factorize phase space abrasion and ablation pieces and closure on target final states

$$\frac{d\sigma}{d\mathbf{p}_F} = \frac{-(2\pi)^4}{\beta} \sum_x \int d\mathbf{q}\, d\mathbf{p}_F \prod_{r=0} d\mathbf{p}_r \sum_{n=1} \prod_{j=1}^{n} \left[d\mathbf{p}_j\right] \delta\left(E_i - E_f\right) \delta\left(\mathbf{p}_i - \mathbf{p}_f\right) |T_{fi}|^2$$

- Factorization solution in terms of abrasion response ftn. For excitation energy ε_{F*}

$$(20) \qquad \frac{d\sigma}{d\varepsilon_{F*}} = \langle T | \int d^2q d^2b d^2b' \quad e^{i\mathbf{q}(\mathbf{b}-\mathbf{b}')} P_{n,n'}(b,b') \Lambda_{n,n'}(q,b,b,E_{F*}) | T \rangle$$

- Ablation (Master equation from Hufner et al.)
  - If $f_b(E,t)$ is the probability of finding the nuclei *b* at time *t* with excitation energy E_b and $P_{kb}(E)$ be the probability that the nuclei, *b* will emit ion *k* with energy *E*, Master equation is $(23) \quad \frac{df^b(E^*_b,t)}{dt} = \sum_j \int dE\, f^a(E^*_a,t) P^a_j(E) - \sum_k \int dE f^b(E^*_b,t) P^b_k(E)$

Isotopic Fragment Production

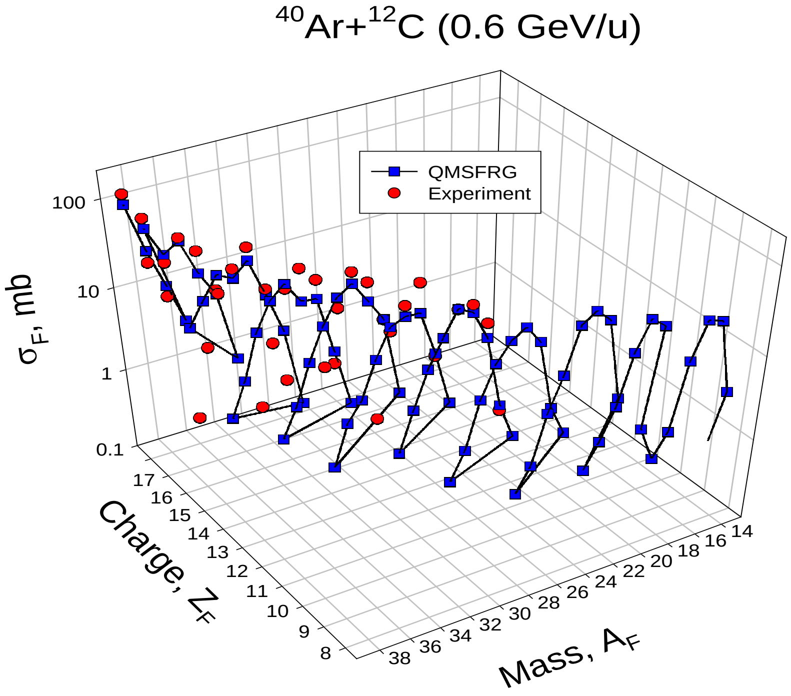

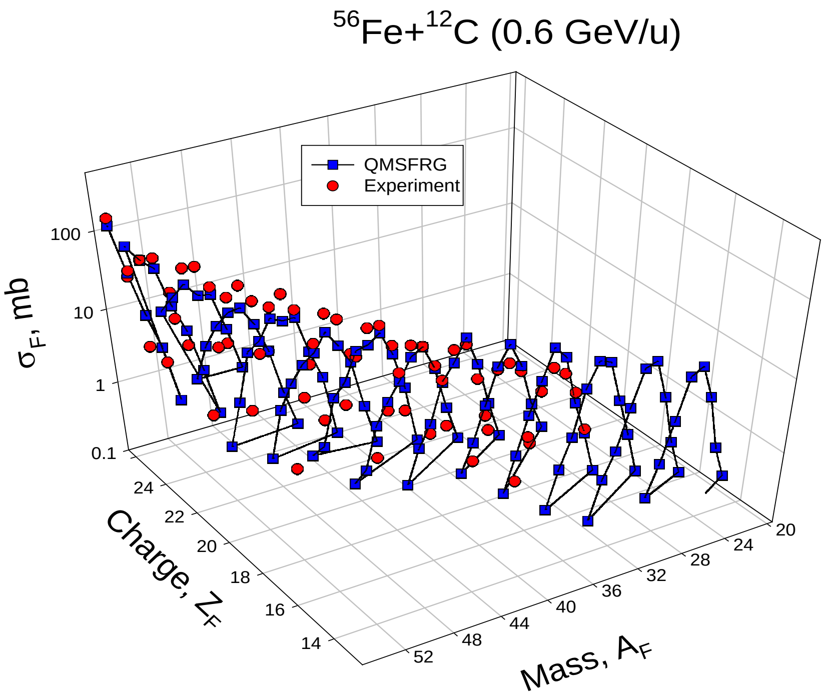

Quantum MS: Iron Fragmentation (+25% Difference Bands)

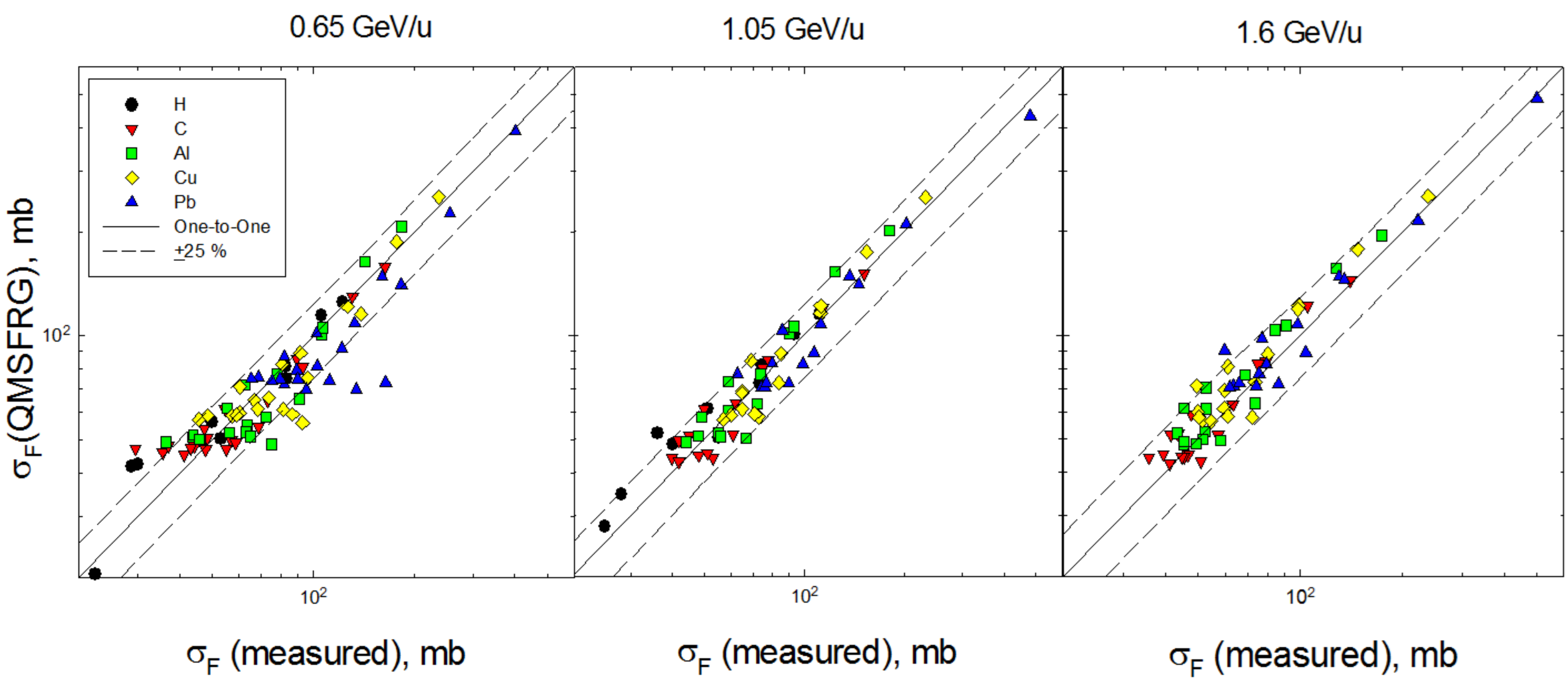

Comparison of QMSFRG model to experimental data for ^{56}Fe fragmentation on several targets at 0.65 GeV/u (Flesch *et al*. (1999)), 1.05 GeV/u (Zeitlin *et al.* (1997)), and 1.6 GeV/u (Cummings *et al.*, 1990).

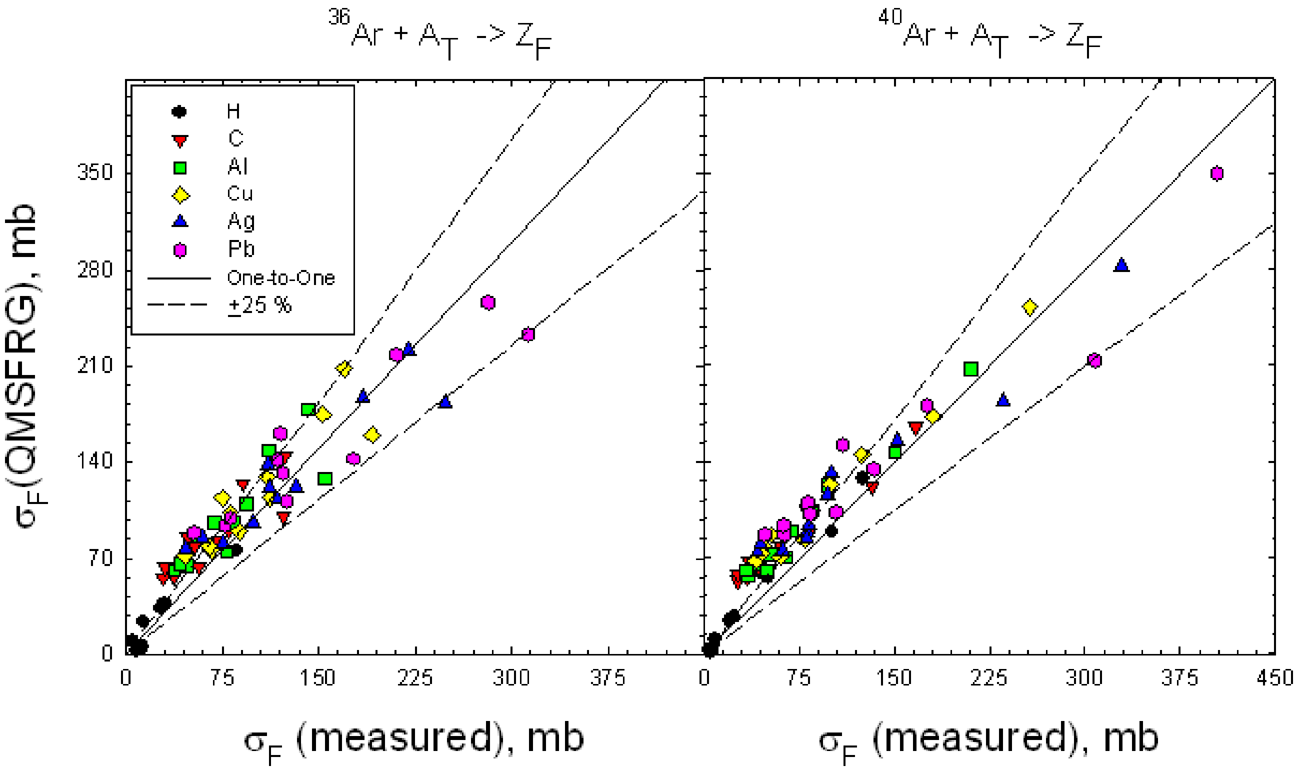

$^{36}Ar + A_T \rightarrow Z_F$
$^{40}Ar + A_T \rightarrow Z_F$
H
C
Al
Cu
Ag
Pb
One-to-One
±25 %
σ_F(QMSFRG), mb
σ_F (measured), mb
0
70
140
210
280
350
0
75
150
225
300
375
450

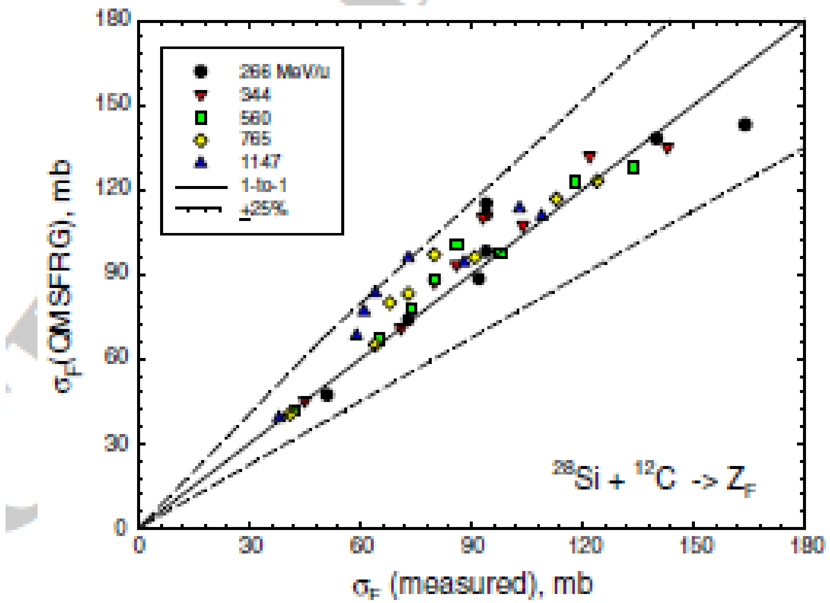

266 MeV/u
344
560
765
1147
1-to-1
±25%
$^{28}Si + ^{12}C \rightarrow Z_F$
σ_F(QMSFRG), mb
σ_F (measured), mb
0
30
60
90
120
150
180

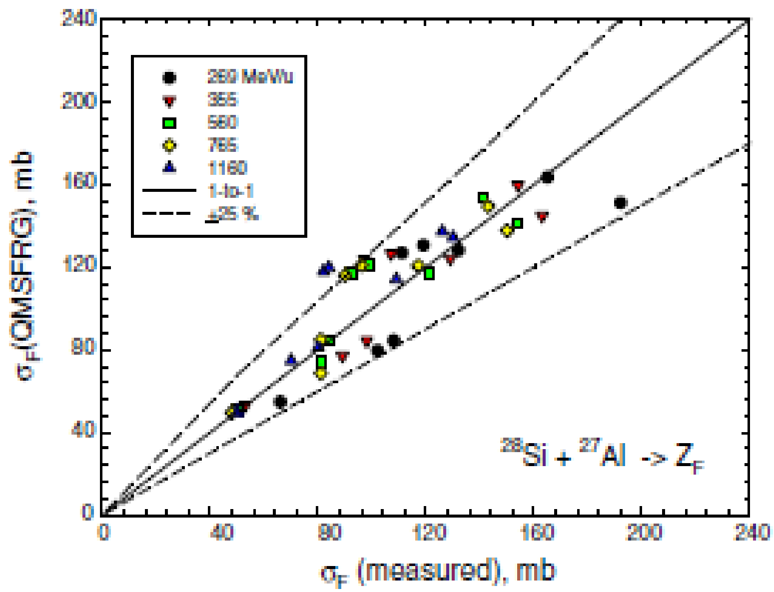

269 MeV/u
355
560
765
1160
1-to-1
±25 %
$^{28}Si + ^{27}Al \rightarrow Z_F$
σ_F(QMSFRG), mb
σ_F (measured), mb
0
40
80
120
160
200
240

Light Ion Fragmentation

Treat as “3-body problem” (Fadeev): Key factors

- High momentum components of wave functions
- P+T->a+b+X; P=(a,b) with spectator contributions from a or b
- Interference terms between a and b amplitudes
- Final state interactions

$$\hat{\mathcal{T}} = \hat{\mathcal{T}}^a + \hat{\mathcal{T}}^b + \hat{\mathcal{T}}^T$$

$$\hat{\mathcal{T}}^a = \hat{T}_{bT} + \hat{T}_{bT}\, G_o(\hat{\mathcal{T}}^b + \hat{\mathcal{T}}^T)$$

$$\hat{\mathcal{T}}^b = \hat{T}_{aT} + \hat{T}_{aT}\, G_o(\hat{\mathcal{T}}^a + \hat{\mathcal{T}}^T)$$

$$\hat{\mathcal{T}}^T = \hat{T}_{ab} + \hat{T}_{ab}\, G_o(\hat{\mathcal{T}}^a + \hat{\mathcal{T}}^b)$$

$$G_o = \left(E - \frac{\mathbf{k}_a^2}{2m_a} - \frac{\mathbf{k}_b^2}{2m_b} - \frac{\mathbf{k}_X^2}{2m_X} + i\eta \right)^{-1}$$

$$\widetilde{T}_{fi}^{(1)} = \widetilde{\phi}(\mathbf{u}_a)\; T_{bX}(\sqrt{s_{bT}}, \mathbf{Q}) + \widetilde{\phi}(\mathbf{u}_b)\; T_{aX}(\sqrt{s_{aT}}, \mathbf{Q})$$

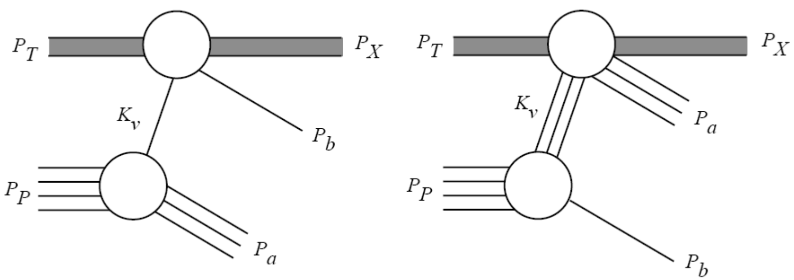

(a) Spectator term. (b) Participant term.

Figure 14. Terms for projectile fragmentation.

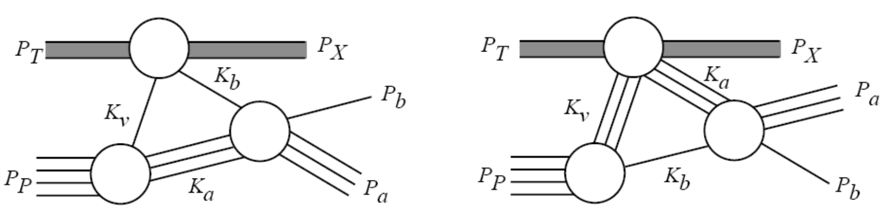

(a) Spectator term. (b) Participant term.

Figure 15. Terms for final-state interaction.

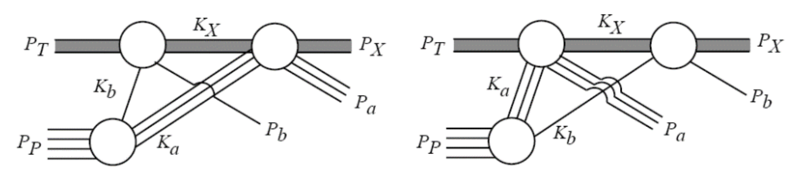

(a) Spectator term. (b) Participant term.

Figure 16. Rescattering corrections.

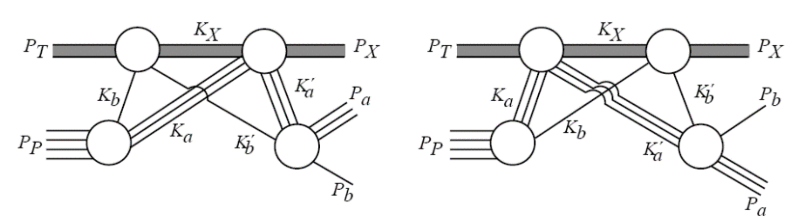

(a) Spectator term. (b) Participant term.

Figure 17. Rescattering corrections with final-state interaction.

Light Ion Fragmentation: interference effects in spectator-participant terms

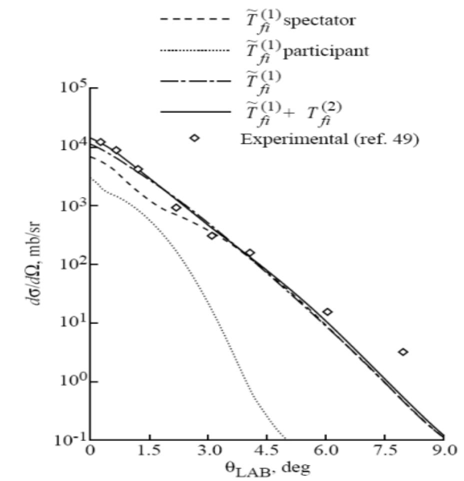

Figure 19. Angular distribution for $\alpha + {}^1H \rightarrow {}^3He$ at 1.02A GeV.

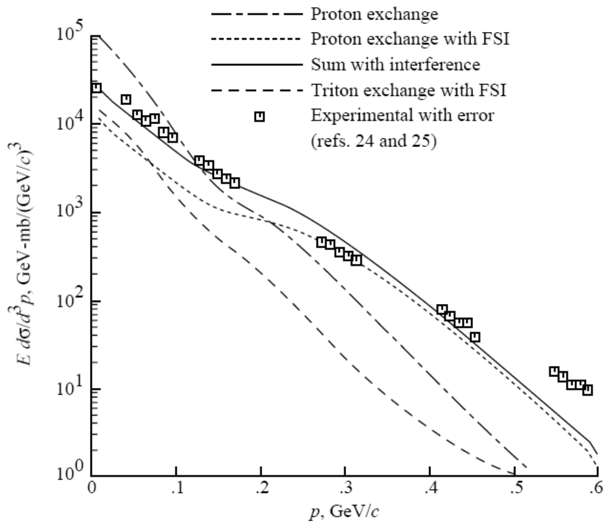

Figure 5. Comparison of calculations of transverse momentum distribution for ^3H production in $^4He + {}^{12}C$ collisions at 0.385 GeV/amu with experimental data.

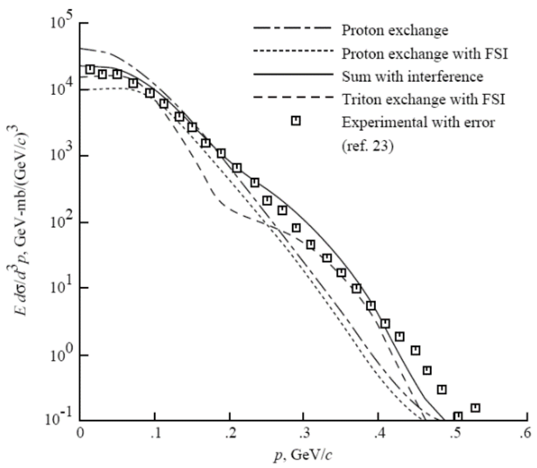

Figure 4. Comparison of calculations of longitudinal momentum distribution for ^3H production in $^4He + {}^{12}C$ collisions at 1.9 GeV/amu with experiment (ref. 23).

Cucinotta Phys Lett B (1992)

^{4}He Fragmentation Energy Dependence

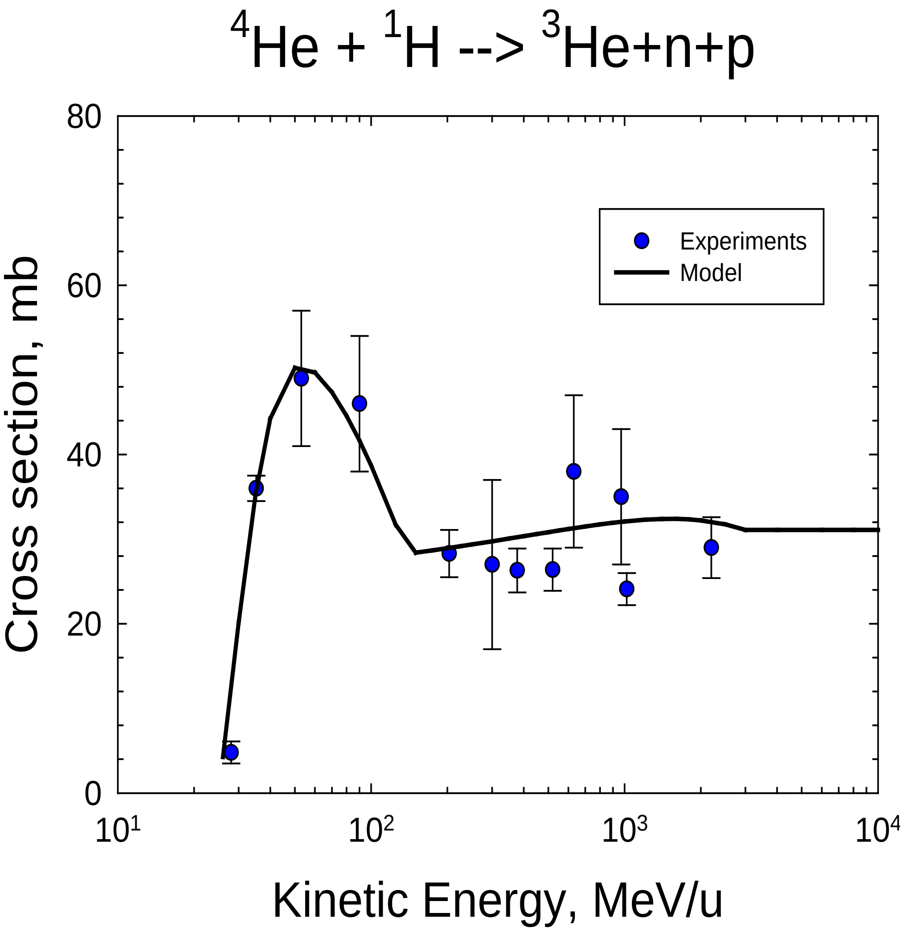

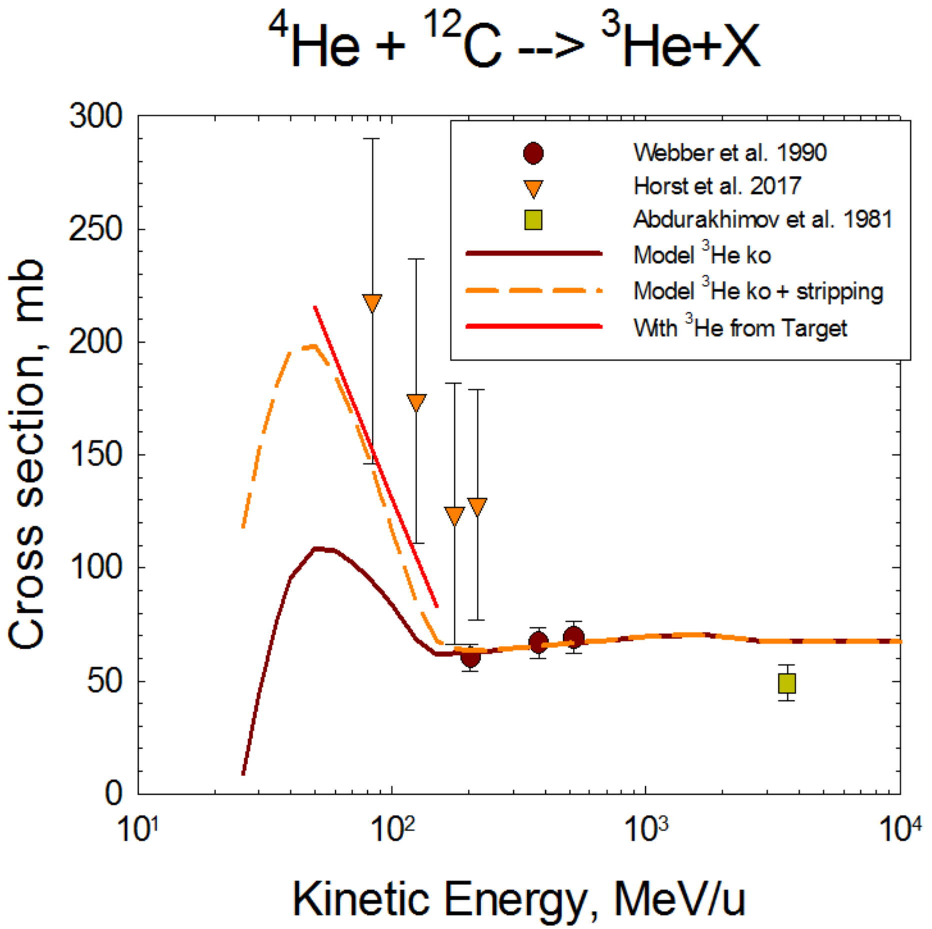

Cluster KO and Coalescence of Light Ions

- Light ions exist as virtual bound state in the nuclear ground state
  - Example 16-O as 4x4He similar for other “4n nuclei”
  - 14-N as virtual 12-C and deuteron, etc.
- Direct ko of lights ions occurs, especially important for H and light targets
- After Hard collisions, if n-nucleons are within defined distance in phase space of each other, then they can coalesce into light ions

$$\left(\frac{d\sigma}{dp}\right)_{LI(A_N)} = C\left(\frac{d\sigma}{dp}\right)^N$$

  - d,t,h,alpha
  - Experimentally the combined abrasion and ablation p and n momentum distribution is described
    - abrasion-ablation separated in time
    - More appropriate to use only abrasion stage distributions for coalescence
  - There is a normalization defect in the popular forms of coalescence model

Production Mechanisms in ^{16}O Fragmentation

^{16}O Fragment	Abrasion	Coalescence	Ablation	EM or α- cluster	Total (mbarns)	Expt. (mbarns)
		A_T=Hydrogen				
n	287.3	0.0	48.3	0.0	284.1	
p	291.4	0.0	70.3	0.1	310.2	
2-H	4.8	29.2	6.3	0.0	40.3	152 ± 23
3-H	2.3	12.7	2.3	0.0	17.3	55 ± 11
3-He	1.2	12.7	3.4	0.0	17.3	55.2 ± 5.7
4-He	61.7	6.6	91.1	9.5	168.9	221 ± 20
		A_T=Carbon				
n	2692.0	0.0	350.5	0.8	2697.0	
p	2781.0	0.0	465.9	1.2	2902.0	
2-H	232.5	196.3	30.8	0.0	459.6	406 ± 36
3-H	17.4	85.3	37.7	0.0	140.4	151 ± 11
3-He	7.2	85.3	11.2	0.0	103.7	136 ± 7.6
4-He	174.4	44.2	218.0	21.0	457.7	474 ± 42
		A_T= Copper				
n	6537.0	0.0	590.6	14.2	6459.0	
p	6889.0	0.0	712.8	21.3	6941.0	
2-H	380.8	386.9	49.7	0.0	817.4	682 ± 72
3-H	27.1	168.0	55.2	0.0	250.3	
3-He	10.6	168.0	16.0	0.0	194.7	
4-He	256.4	87.1	316.5	35.7	695.6	748 ± 80

e.g. Ablation Multiplicities: ^{16}O to ^{10}B

Af	Zf	N1	N2	N3	Sigma, mb
10	4	1	1	2	3.16E-02
10	4	1	1	7	2.96E-01
10	4	1	2	1	5.33E-02
10	4	1	2	2	4.08E-02
10	4	1	2	3	1.07E-02
10	4	1	2	5	1.32E-03
10	4	1	2	7	2.58E-01
10	4	1	3	2	1.25E-02
10	4	1	3	7	9.58E-02
10	4	1	5	2	3.11E-03
10	4	1	5	7	2.42E-02
10	4	1	7	7	1.24E-01
10	4	2	1	1	8.31E-02
10	4	2	1	2	3.34E-02
10	4	2	1	3	1.06E-02
10	4	2	1	5	1.95E-03
10	4	2	1	7	3.17E-01
10	4	2	2	1	2.41E-02
10	4	2	2	2	4.91E-02
10	4	2	2	3	1.54E-02
10	4	2	2	4	4.36E-03
10	4	2	2	5	1.77E-03
10	4	2	2	7	1.10E-01
10	4	2	3	1	1.94E-02
10	4	2	3	2	1.82E-02
10	4	2	3	3	6.62E-03
10	4	2	3	7	6.02E-02
10	4	2	4	2	4.52E-03
10	4	2	4	7	4.41E-02
10	4	2	5	1	3.53E-03
10	4	2	5	2	4.15E-03
10	4	2	5	7	3.41E-02
10	4	2	6	7	7.56E-01
10	4	2	7	7	1.89E-01
10	4	3	1	2	1.61E-02
10	4	3	1	7	1.65E-01
10	4	3	2	1	2.55E-02
10	4	3	2	2	2.98E-02
10	4	3	2	3	5.37E-03
10	4	3	2	7	9.23E-02
10	4	3	3	2	6.18E-03
10	4	3	3	7	5.56E-02
10	4	3	5	7	8.11E-03
10	4	3	7	7	4.47E-01
10	4	4	2	2	5.03E-03
10	4	4	2	7	3.86E-02
10	4	4	7	7	1.98E-01
10	4	5	1	2	3.91E-03
10	4	5	1	7	4.85E-02
10	4	5	2	1	3.39E-03
10	4	5	2	2	6.87E-03
10	4	5	2	7	5.25E-02
10	4	5	3	7	1.34E-02
10	4	5	7	7	1.70E-01
10	4	6	2	7	1.19E-01
10	4	6	7	7	2.82E+00

N1= type j=1,7 (n,p,d,t,h,α,0) emission in ablation step-1; etc

Conclusions

- Event based transport models are of interest to support event based biological models.
  - High multiplicity events in tissues (especially Target Fragments).
  - Couple Monte-Carlo Track models to nuclear processes.
  - Time dependence of events in tissue for chronic exposure.
- 2nd Order Optical model improves agreement with expt. for Inelastic cross sections to ~5% for p, n, Heavy ions.
  - Pion inelastic about ~10%.
  - Model agreement to Expt. similar to Expt. To Expt. agreement.
- Quantum M.S. is in good agreement with heavy ion fragmentation cross sections for GCR nuclei ($\pm$25%).
  - Expt. to Expt. agreement about 15% so would be useful for further improvements in fragmentation models to 15%.
- A bottle-neck for MC codes is calculating or sampling light particle energy/angles.
  - New approaches to defining parametric libraries and algorithms to sample spectra are needed to improve CPU times.
  - 2- to n-particle Correlation spectra as a measure of event accuracy.

Other Material

NASA Radiation Quality Function (QF)

- Maximum effectiveness per particle can be estimated by experiments for RBE_{max} and occurs at "saturation point" of cross section for any Z
- Delta-ray effects for relativistic particles accounted for in QF model; higher Z less effective at fixed LET compared to lower Z:

$$Q_{NASA} = (1 - P(Z,E)) + \frac{6.24(\Sigma_0 / \alpha_\gamma)}{LET} P(Z,E)$$

$$P(Z,E) = (1 - \exp(-Z^{*2} / \kappa\beta^2))^m P_{TD}$$

- PDFs account for variation of three parameters values:

(Σ_0 / α_γ, m, and κ) based on existing but limited radiobiology data. PTD low energy correction. Qmax~ Σ_0 / α_γ

- Monte-Carlo propagation of uncertainties using PDF's for epidemiology, QF, transport physics, dose-rate, etc.

Heavy Ion Multiple Scattering (MS)

- Two-body t-matrix in nucleus medium $\tau_{\alpha j} = v_{\alpha j} + v_{\alpha j}\, G\, \tau_{\alpha j}$
- Two-body t-matrix for free NN scattering $t'_{\alpha j} = v_{\alpha j} + v_{\alpha j}\, g\, t'_{\alpha j}$
- Major difficulty is Many-body Operator G
- Define Moller operator that transforms system up to the α and j collision (1): $\omega_{\beta j} = 1 + \Sigma_{(\beta k) ne (\alpha j)}\, G\, \tau_{\beta k}\, \omega_{\beta k}$
- Define Moller operator that transforms up to α and j plus additional contributions due to α and j constituents (2): $\Omega = \omega_{\alpha j} + G\, \tau_{\alpha j}\, \omega_{\alpha j}$
- Substituting $\Omega = 1 + \Sigma_{\alpha j} G\, \tau_{\alpha j}\, \omega_{\alpha j}$ Can show $v_{\alpha j}\, \Omega = \tau_{\alpha j}\, \omega_{\alpha j}$
- Or $T = \Sigma\, v_{\alpha j}\, \Omega = \Sigma\, \tau_{\alpha j}\, \omega_{\alpha j}$
- Still a complicated Many-body problem but for high-energy scattering the <u>Impulse Approximation</u> is valid-
  - Full Green's function Defined by $(E - H_P - H_T) G = 1$
  - Free Green's function Defined by $(E - \Sigma T_j - \Sigma T_\alpha) G_0 = 1$
- Implementation of Impulse Approx. define

$$t_{\alpha j} = v_{\alpha j} + v_{\alpha j}\, G_0\, t_{\alpha j}$$

- One can show (3): $\tau_{\alpha j} = t_{\alpha j} + t_{\alpha j}\, (G - G_0)\, \tau_{\alpha j}$
- Impulse approximation is then $\tau_{\alpha j} \sim t_{\alpha j}$
- Formal approach to study corrections to impulse approximation can be made using (3)

Elastic and Inclusive Projectile
P+T→ P+T and P+T→ P+X

$$\left.\frac{d\sigma^{PT}}{d\Omega}\right)_{IN} = \left.\frac{d\sigma}{d\Omega}\right)_{TOT} - \left.\frac{d\sigma}{d\Omega}\right)_{EL} - \left.\frac{d\sigma^{P}}{d\Omega}\right)_{IN} - \left.\frac{d\sigma^{T}}{d\Omega}\right)_{IN}$$

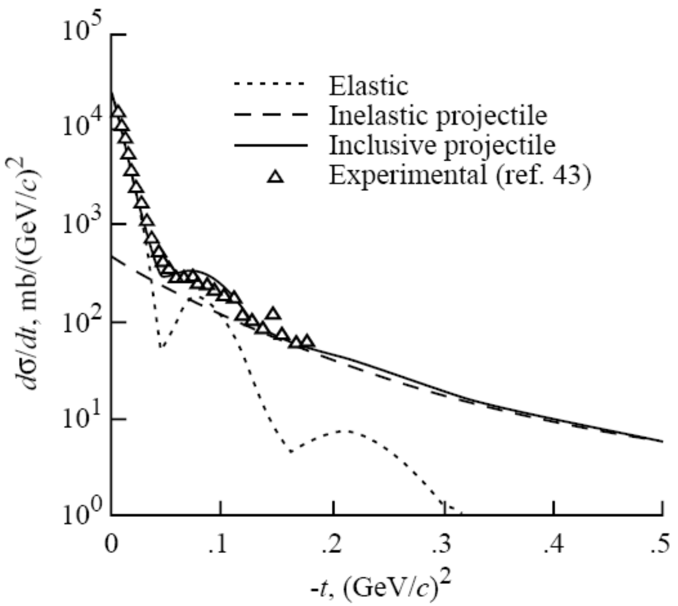

Figure 9. Inclusive ^{4}He+^{12}C scattering distributions at 3.6A GeV versus invariant momentum transfer.

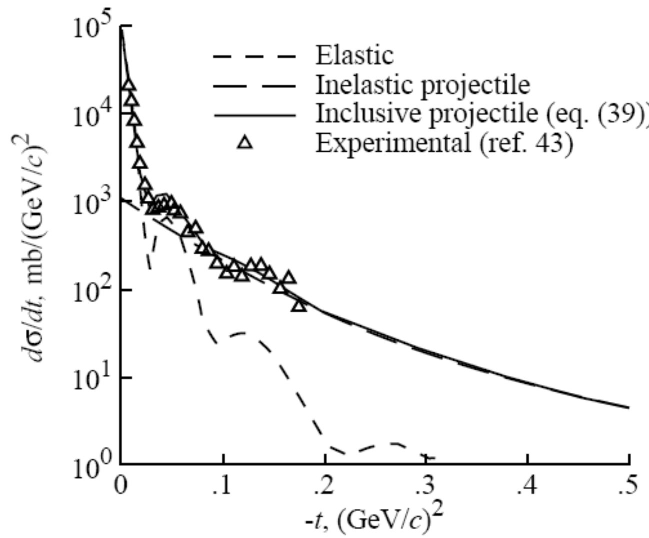

Figure 10. Inclusive ^{4}He+^{27}Al scattering distributions at 3.6A GeV versus invariant momentum transfer.

$$\left.\frac{d\sigma}{d\Omega}\right)_{IN} \cong \left(\frac{k}{2\pi}\right)^2 \int d^2b\, d^2b'\, e^{i\boldsymbol{q}\cdot(\boldsymbol{b}-\boldsymbol{b}')} e^{i\left(\chi(\boldsymbol{b})-\chi^{+}(\boldsymbol{b}')\right)} \left(e^{\Upsilon(\boldsymbol{b},\boldsymbol{b}')} - 1\right)$$

$$\left.\frac{d\sigma^{P}}{d\Omega}\right)_{IN} \cong \left(\frac{k}{2\pi}\right)^2 \int d^2b\, d^2b'\, e^{i\boldsymbol{q}\cdot(\boldsymbol{b}-\boldsymbol{b}')} e^{i\left(\chi(\boldsymbol{b})-\chi^{+}(\boldsymbol{b}')\right)} \left(e^{\Omega(\boldsymbol{b},\boldsymbol{b}')} - 1\right)$$

Cucinotta et al., J.Phys G (1992)

Nucleon-Nucleon (NN) Scattering:

1^{st} order Optical Model independent of Ratio of Real to Imaginary part of NN Amplitude (α_{NN}). 2^{nd} Order and Energy/Momentum spectra are not independent.

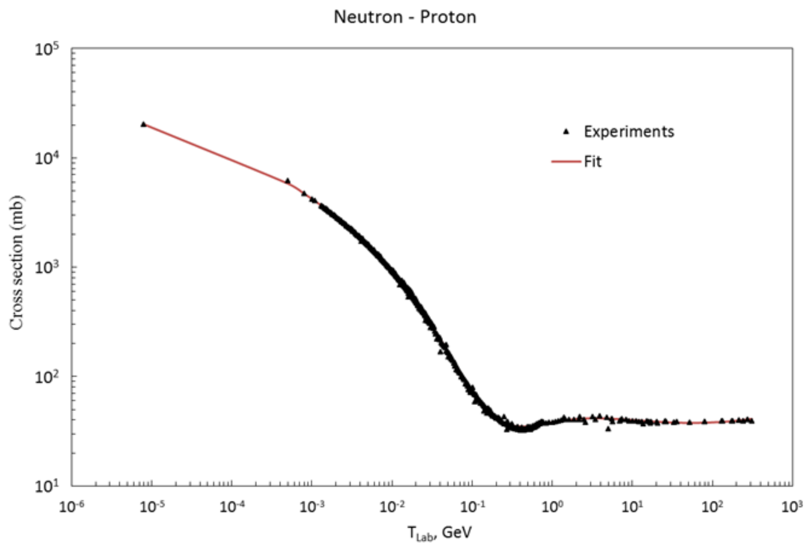

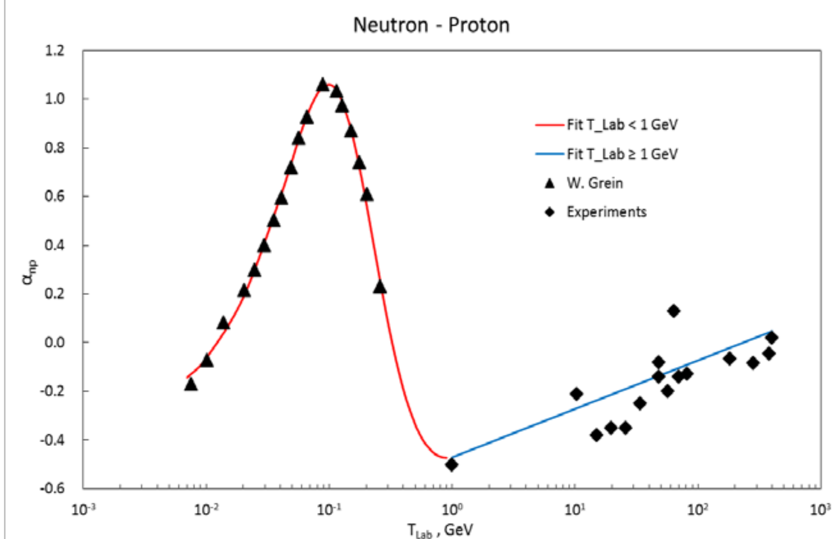

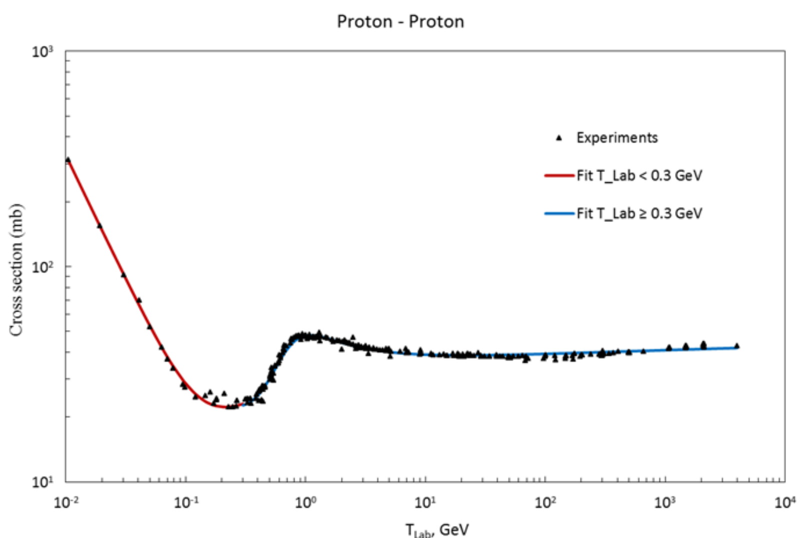

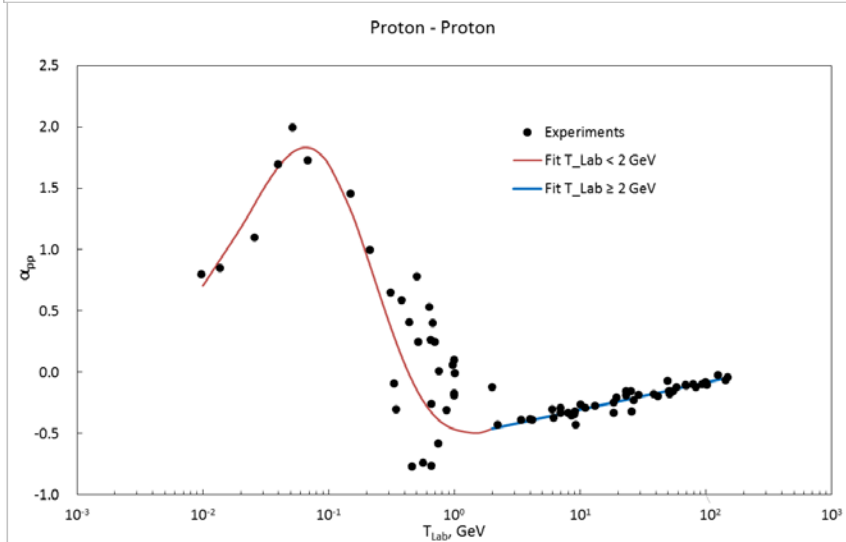

GCR Environment Model

- Local Inter-stellar Spectra (LIS) (Leaky Box Model)

$$q_i + \sum_j \varphi_j \left(\frac{1}{\Lambda_{ji}^{\text{spall}}} + \frac{1}{\Lambda_{ji}^{\text{decay}}} + \frac{1}{\Lambda_{ji}^{\delta Q}} \right) = \varphi_i \left(\frac{1}{\Lambda_i^{\text{spall}}} + \frac{1}{\Lambda_i^{\text{decay}}} + \frac{1}{\Lambda_i^{\delta Q}} + \frac{1}{\Lambda_i^{\text{esc}}} \right) - \frac{d(w_i \varphi_i)}{d\varepsilon}.$$

- Modification of CRIS Leaky Box model (George et al. 2009; Lave et al., 2013)

$$F_{LIS}(Z,E) = \frac{F_0 E^{-\gamma}}{[1+(E_1/E)^{\alpha_1} + (E_2/E)^{\alpha_2}]}$$

$$\gamma(E) = \gamma_0 + \gamma_1 [1 - e^{-(E/15000)}]^2$$

- Parker Theory of Solar Modulation